Pure & Appl. Chem., Vol. 62, No. 9, pp. 1661–1666, 1990.
Printed in Great Britain.
© 1990 IUPAC

Plasma deposition of semiconductor multilayer structures

Masataka Hirose and Seiichi Miyazaki

Department of Electrical Engineering, Hiroshima University
Higashi-Hiroshima 724, Japan

Abstract The early stages of thin film growth from the rf glow discharge of silane-based gas mixtures have been systematically studied by structural characterizations of the silicon based multilayers. The x-ray diffraction, its rocking curve and x-ray interference of hydrogenated amorphous silicon(a-Si:H, 10 ∿ 200 A thick)/stoichiometric silicon nitride (a-Si_3N_4:H, 25 ∿ 250 A) multiple layers have been carefully measured. The results indicated that the amorphous silicon/silicon nitride interface is atomically abrupt and the thicknesses of the respective layers are atomically flat regardless of substrate materials. This demonstrates that the precursors impinging onto a substrate from the gas phase homogeneously cover the growing surface and layer by layer growth proceeds on atomic scale. In the plasma deposition of the covalently bonded semiconductors and insulators studied in the present experiments, the island formation on a substrate at the beginning of thin film growth is very unlikely. The extremely flat features of the ultra thin multilayer structures are also confirmed by observing the quantum size effects in the amorphous silicon/silicon nitride system.

INTRODUCTION

Plasma enhanced chemical vapor deposition (CVD) is composed of sequential steps of the electron impact dissociation of material gases, transport of the reaction products onto the surface, their surface condensation, network propagation reaction and the desorption of surface products. Recent extensive studies on the gas phase chemistry of a silane plasma have indicated that the major stable precursor is most likely to be SiH_3 (ref. 1-4). The surface processes during a-Si:H film growth have also been studied by ellipsometry (ref. 5) and infrared modulation spectroscopy (ref. 6). The latter result has shown the existence of SiH_3 molecular units on the surface, suggesting the very thin surface layer whose chemical composition is basically different from the underlying a-Si:H matrix. The ellipsometric study has revealed the presence of a rather low density surface layer or the possibility of island growth (ref. 5). More recently Collins (ref. 7) has observed the spatially homogeneous growth mode and island growth depending upon the substrate surface materials and probably upon deposition conditions. Many years ago Knights (ref. 8) proposed an a-Si:H growth model, in which substrate-dependent nucleation is followed by growth of islands until island boundaries are in close proximity. This model is also widely known in the case of metal deposition. Now, questions to be answered are what is happening on atomic scale at the beginning of a-Si:H growth and whether the island growth or atomic layer growth is more predominant mode in the deposition. This paper reviews the recent results on the plasma deposition and characterizations of a-Si:H/a-Si_3N_4:H superstructures and new insights on the early stages of the thin film growth.

EXPERIMENTAL

Well defined multilayers consisting of a-Si:H (10 - 200 A) and a-Si_3N_4:H (25 - 200 A) have been grown on chemically cleaned crystalline Si(100), 100 A thick thermally grown SiO_2/Si(100) and Cr (typically 100 A and 1100 A thick)/Si(100) substrates. The detailed technique of the multilayer growth has been reported in Ref. 9. Monosilane gas diluted to 10.3 % in H_2 was used for a-Si:H deposition and SiH_4(10.3% in H_2) + pure NH_3 with a molar fraction of $[NH_3]/[SiH_4]$ = 10 for stoichiometric a-Si_3N_4:H. The substrate temperature, the gas pressure and the rf power density were maintained at 300 °C, 0.2 Torr and 32 mW/cm^2, respectively. The rf power was turned off at each step of the respective layer deposition. Also, for eliminating the undesirable nitrogen incorporation into a-Si:H after a-Si_3N_4:H deposition, the reaction chamber was pumped down to ∿10^{-3} Torr and carefully purged with H_2 and SiH_4. The growth rate was kept at 0.27 A/sec for a-Si:H and 0.42 A/sec for a-Si_3N_4:H. The residence time of gases in the reactor was about 2 sec, being short enough compared with the monolayer growth time. The x-ray interference pattern of an a-Si:H/a-Si_3N_4:H multilayer

was recorded with a conventional Θ - 2Θ diffractometer using filtered CuKα(λ = 1.5418 A) x-rays.

RESULTS AND DISCUSSION

1. Microstructure of A-Si:H/a-Si_3N_4:H multilayers

1.1 X-ray diffraction

Periodic structures in amorphous superlattices have been evaluated by using Auger electron spectroscopy (AES), x-ray photoelectron spectroscopy (XPS), x-ray diffraction and transmission electron microscopy (ref. 10-13). Observation of sharp x-ray diffraction peaks in amorphous multilayers clearly indicates the existence of well defined superstructures (Fig 1). As shown in the figure the layer spacing determined from the Bragg diffraction angles is generally in excellent agreement with the layer thickness estimated from the deposition rate of the individual layer.

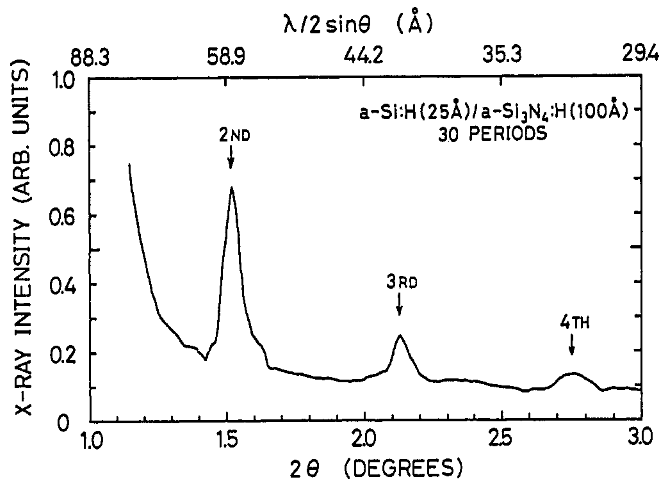

Fig. 1. X-ray diffraction intensity vs scattering angle (lower scale) and lattice spacing (upper scale) for an a-Si:H(25 A)/a-Si_3N_4:H(100 A) multilayer.

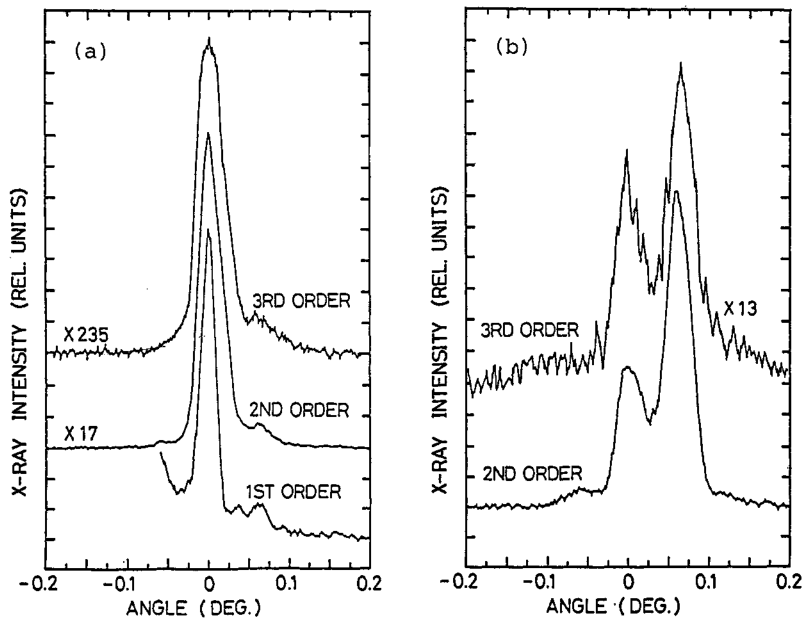

Fig. 2. X-ray rocking curves for a plasma CVD a-Si:H(25 A)/a-Si_3N_4:H(100 A) superlattice measured by aligning the sample at the main Bragg peak (a) and the subpeak (b).

The measured full width at half maximum (FWHM) for a-Si:H/a-Si_3N_4:H multilayers is less than 0.1 degree, indicating that the deposited layers are smooth and parallel on atomic scale (ref. 13). For extracting further information on the layered structure x-ray rocking curves have been measured as shown in Fig. 2 (a). The sharp peak with an FWHM of less than 0.04 degrees strongly supports the abrupt interface which enables us to observe quantum size effects. In the figure, however, there exists a weak satellite peak at about +0.06 degrees away from the main peak. This subpeak becomes more significant in the rocking curve taken by optically aligning the sample at +0.06 degrees as shown in Fig. 2 (b). This subsidiary peak appears at the position independent of the diffraction order, implying that the superlattice contains local mosaic structure. As observed by the transmission electron micrograph of a-Si:H/a-SiC:H (ref. 14) and a-Si:H/a-Ge:H (ref. 13) multilayers, the surface morphology becomes worse and undulated as the number of deposited layers is increased. This is a possible cause of the local mosaic structure.
In addition to this, the other weak peak is observed in Fig. 2 (a) at +0.03 degrees in the first order diffraction. Also, in the 3rd order diffraction a small peak centered at +0.09 degrees seems to be existing in the tail of satellite signal (see Fig. 2 (a) and (b)). This suggests the presence of monolayer steps in the superlattices (ref. 13). Such monolayer steps might arise from difference in the initial stages of a-Si:H growth on a-Si_3N_4:H and a-Si_3N_4:H growth on a-Si:H. In fact, when an a-Si:H layer is exposed to an NH_3 plasma, the a-Si:H surface is rapidly nitrided (ref. 15). Therefore, a highly NH_3 rich silane plasma in contact with the a-Si:H surface simultaneously promotes a-Si_3N_4:H deposition and a-Si:H nitridation at the beginning of overgrowth. This could induce local atomic steps even though the a-Si:H surface is ideally flat.
In the current x-ray diffraction study the multilayers more than 20 periods were used to obtain the Θ - 2Θ curves. However, such structure induces the problem of undulation in the deposited layer. In order to clarify the very early stages of deposition, we have also measured the x-ray interference patterns of the multilayer whose number of periods is in the range of 5 to 20, and the results have been compared with the theoretical analysis.

1.2 X-ray interference

An x-ray diffraction pattern from a finite number of scattering layers is predicated by a dynamical theory (ref. 16) which takes into account the reflections at the multilayer-air and multilayer-substrate interfaces. This dynamical approach is analogous to that employed in the design of optical interference filters and is based on the Fresnel equations. The specularly reflected intensity by the ideal multilayer consisting of N stratified homogeneous laminas with the atomically abrupt interface can be computed by the recursion formula. The detail of analysis is reported elsewhere (ref. 17).
The typical x-ray interference spectrum observed for five periods of a-Si:H(20 A)/a-Si_3N_4:H(50 A) multilayer is shown in Fig. 3, where the interference patterns together with sharp Bragg peaks are observed. The calculated spectra corresponding to the sample of Fig. 3 are shown in Fig. 4. The best fit of the calculated result to the measured curve in Fig. 3 yields an a-Si:H well width of 22 A and an a-Si_3N_4:H barrier thickness of 49 A. The layer thickness determined by the growth rate of each layer is in excellent agreement with the calculated result. The calculated spectrum well reproduces the measured interference pattern not only in its intensity but also in the full width at half maximum of the diffraction peaks. This indicates that the a-Si:H/a-Si_3N_4:H interface is abrupt on atomic scale and that the respective layers are defined to be atomically flat and parallel to each other.

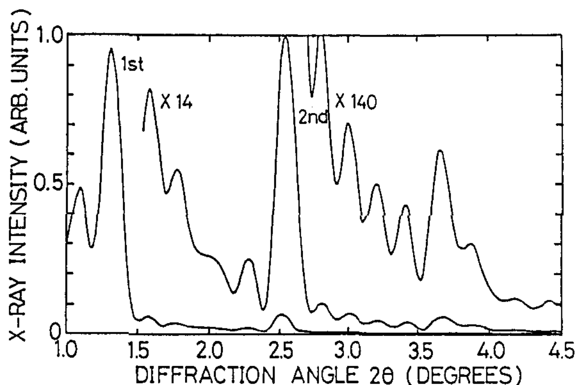

Fig. 3. X-ray diffraction patterns for the multilayer with a designed well width of 20 A a-Si:H and a barrier thickness of 50 A.

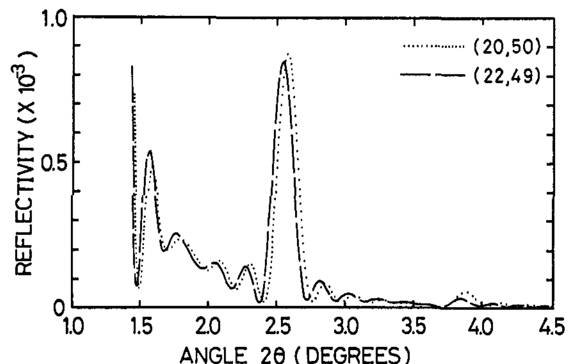

Fig. 4. Calculated reflectivities for the respective multilayer thickness denoted by the numbers in the parentheses (d_S, d_N), where d_S is the a-Si:H layer thickness and d_N the a-Si_3N_4:H in angstroms.

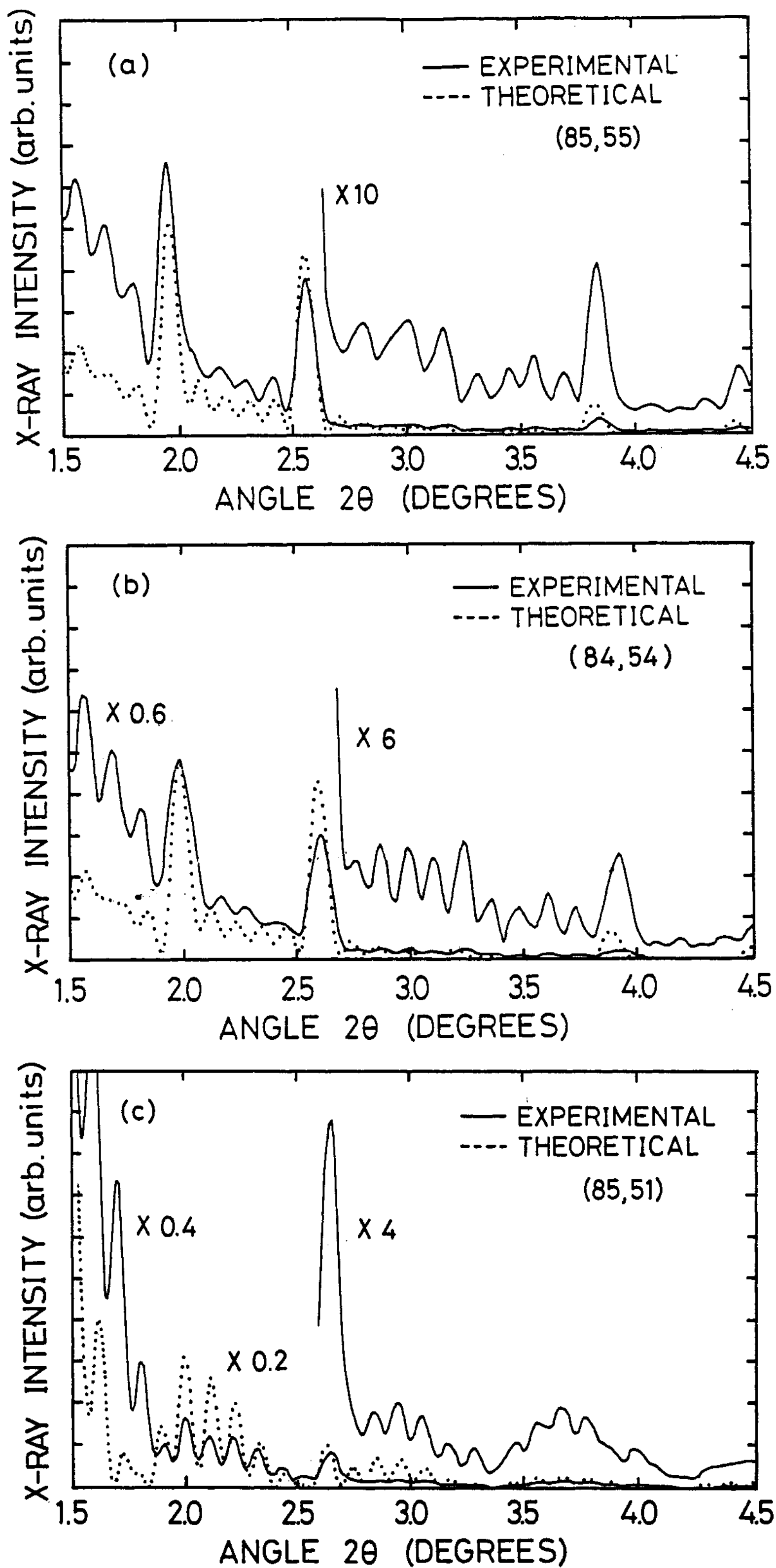

Fig. 5. Measured and calculated x-ray interference patterns for a-Si:H/a-Si_3N_4:H superlattice with 5 periods grown on (a) c-Si(100), (b) SiO_2 (100 Å thick)/Si(100) and (c) Cr (100 Å thick)/Si(100) substrates. The value in the parentheses denotes the a-Si:H and a-Si_3N_4:H thickness employed for the calculation.

2. Substrate dependence

The x-ray diffraction and interference measurements in the previous section were carried out by using multilayers grown on semiconducting c-Si(100) substrates. In the plasma deposition the charged particles impinge onto a grounded substrate and hence the surface potential is more or less dependent on the nature of substrate material; i.e., semiconductor, insulator and metal. Also, the nucleation reaction at the beginning of deposition is possibly influenced with the chemical properties of substrate surfaces. In this sense, the multilayer growth on semiconductor, insulator and metal has been comparatively investigated by using the x-ray interference technique. Figure 5 represents typical x-ray interference spectra measured for 5 periods of multilayers grown on the three different kinds of substrates together with the theoretical analysis. Basically interference patterns coincide well with the theoretically predicted ones. It is interesting to note that the half width at half maximum of the Bragg peaks tends to be broadened on the insulating substrate. Nevertheless, the results indicate that the early stages of a-Si:H growth is basically independent of the nature of substrates as far as the present experimental conditions are concerned.

3. Structural stability

The a-Si:H/a-Si_3N_4:H interface is found to be atomically abrupt and the respective layer is extremely flat on atomic scale. However, the Si-Si bond length (2.35 A) is significantly larger than that of Si-N (1.89 A). This must introduce significant amount of internal stress in the interface region, the part of which could be relaxed by increasing Si and N bond angle fluctuations in the amorphous network as shown by Raman scattering (ref. 18). The thermal stability of this system has been tested by annealing the multilayer at temperatures more that 800 °C as shown in Fig. 6. The a-Si:H layer thinner than 50 A never crystallized at a temperature of 800 °C, while a-Si:H thicker than 100 A resulted in partial crystallization, in consistence with the crystallization temperature of a-Si:H at about 650 °C. This significant increase of crystallization temperature might be due to the existence of thermally stable a-Si_3N_4:H barriers whose influence propagates into a-Si:H network being away from the interface by more than 12 A.

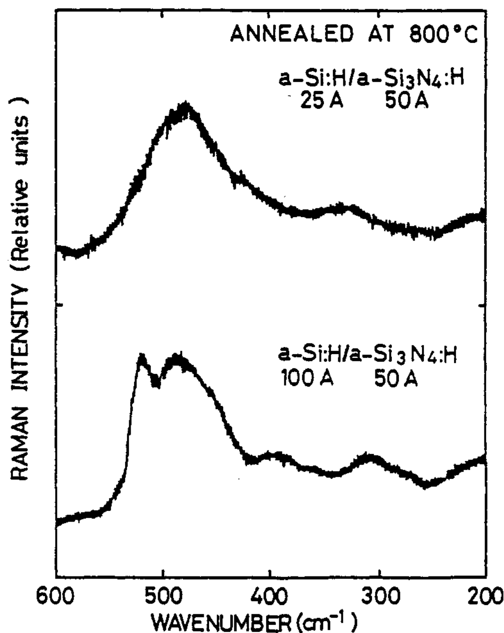

Fig. 6. Raman spectra for superlattices with 25 and 100 A thick a-Si:H well layers. The thickness of a-Si_3N_4:H barrier layer is fixed at 100 A.

4. Quantum size effects

The subband formation in a very narrow (10 - 40 A thick) a-Si:H potential well sandwiched by a-Si_3N_4:H barriers has been directly demonstrated by observing the resonant tunneling of the a-Si:H/a-Si_3N_4:H double barrier structures (ref. 19). More recently, it has been reported that the optical absorption spectrum exhibits fine structures reflecting the density of states in the subband (ref. 20).

The energy of the quantized state is extremely sensitive to the fluctuation of the a-Si:H well width as shown by the following equation:

$$\Delta En/En = 2\Delta L/L \quad (1)$$

Here, L and ΔL is the well width and its fluctuation, respectively, and En and ΔEn is the subband energy and its broadening. Now suppose L = 30 A and ΔL = 3 A, then $\Delta En/En$ = 20 %. Therefore, the quantized states can be experimentally detected only when the a-Si:H well width is controlled on atomic scale. From the successful observation of the quantum size effects, we may conclude that spatially homogeneous growth of a-Si:H proceeds on the surface.

CONCLUSIONS

The plasma deposition of covalently bonded amorphous semiconductor thin films proceeds through spatially homogeneous atomic layer growth as demonstrated by x-ray diffraction and interference measurements. Also, the ultra thin layer is atomically flat and the interface is abrupt on atomic scale, regardless of the nature of substrates. It is very unlikely to assume that the island growth and its coalescence takes place at the beginning of the plasma deposition. The semiconductor multilayer structures are thermally stable compared to the bulk phase, and the quantum confinement of carriers in the semiconductor potential well offers the capability of designing and synthesizing new materials with novel electronic properties (ref. 21-23).

Acknowledgement

This work was partly supported by a Grant-in-Aid for Scientific Research on Reactive Plasma in Priority Areas from the Ministry of Education, Science and Culture.

REFERENCES

1. A. Matsuda and K. Tanaka, J. Appl. Phys., 60 2351 (1986).
2. N. Itabashi K. Kato, N. Nishiwaki, T. Goto, C. Yamada and E. Hirota, Jpn. J. Appl. Phys., 27 L1565 (1988).
3. A. Gallagher and J. Scott, Annual report to SERI for contacts Nos. XB-2-02085-1 and DB-2-02189-1, Solar Energy Research Institute, Golden, Colorado (1983).
4. P. A. Longway and F. W. Lampe, J. Phys. Chem., 87 354 (1983).
5. R. W. Collins and J. M. Cavase, J. Non-Cryst. Solids, 97 & 98 269 (1987).
6. T. Wadayama, W. Suetaka and A. Sekiguchi, Jpn. J. Appl. Phys., 27 501 (1988).
7. R. W. Collins, Private Communication.
8. J. C. Knihts, J. Non-Cryst. Solids 35 & 36 159 (1980).
9. M. Hirose, N. Murayama, S. Miyazaki and Y. Ihara, Proc. of Material Research Society Symp. 70, Palo Alto, pp.405-414 (1986).
10. B. Abeles and T. Tiedje, Phys. Rev. Lett. 51 2003 (1983).
11. J. Kakalios, H. Fritzche, N. Ibaraki and S. R. Ovshinsky, J. Non-Cryst. Solids 66 339 (1984).
12. S. Miyazaki, N. Murayama, M. Hirose and M. Yamanishi, Technical Digest of the 1st Intern. Photovoltaic Science and Engineering Conf. (Kobe, 1984) p. 425.
13. B. Abeles, T. Tiedje, K. S. Liang, H. W. Deckman, H. C. Stasiewsky, J. C. Scanlon and P. M. Eisenberger, J. Non-Cryst. Solids 66 351 (1984); M. Hirose, N. Murayama. S. Miyazaki and Y. Ihara, Proc. of Mat. Res. Soc. Symp. 70 p. 405 (1986).
14. H. Itoh, S. Matsubara, S. Muramatsu, N. Nakamura and T. Shimada, Technical Digest of the 3rd Intern. Photovoltaic Science and Engineering Conf. Tokyo, p. 37 (1987).
15. Y. Hazama, K. Yamada, S. Miyazaki and M. Hirose, J. Non-Cryst. Solids, to be published.
16. L. G. Parratt, Phys. Rev., 95 359 (1954).
17. S. Miyazaki, Y. Kohda, Y. Hazama and M. Hirose, J. Non-Cryst. Solids, to be published.
18. S. Miyazaki, Y. Ihara and M. Hirose, J. Non-Cryst. Solids 97 & 98 887 (1987).
19. S. Miyazaki, Y. Ihara and M. Hirose, Phys. Rev. Lett. 59 125 (1987).
20. K. Hattori, T. Mori, H. Okamoto and Y. Hamakawa, Phys. Rev. Lett. 60, 825 (1988).
21. H. Tarui, M. Matsuyama, S. Tsuda, Y. Hishikawa, T. Takahama, S. Nakayama, N. Nakamura, T. Fukatsu, S. Nakano, M. Ohnishi and Y. Kuwano, Extended Abstracts of the 6 th Intern. Conf. on Solid State Devices and Materials, Tokyo, p. 687 (1986).
22. S. Miyazaki, N. Murayama and M. Hirose, J. Non-Cryst. Solids 77 & 78 1089 (1985).
23. M. Tsukude, S. Hata, Y. Kohda, S. Miyazaki and M. Hirose, J. Non-Cryst. Solids 97 & 98 317 (1987).